Testicular Damage by Microcirculatory Disruption and Colonization of an Immune-privileged Site during *Borrelia crocidurae* Infection

By Alireza Shamaei-Tousi,* Ola Collin,‡ Anders Bergh,§ and Sven Bergström*

*From the *Department of Microbiology, the ‡Department of Anatomy, and the §Department of Pathology, Umeå University, SE-901 87 Umeå, Sweden*

Abstract

The agent of African relapsing fever, *Borrelia crocidurae*, causes reversible multiple organ damage. We hypothesize that this damage is caused when the spirochete forms aggregate with erythrocytes in vivo, creating rosettes that plug the microcirculatory system. To test this hypothesis, we compared testicular microcirculation over an extended time period in two groups of rats: one experimentally inoculated with *B. crocidurae*, the other with the nonerythrocyte rosette–forming *Borrelia hermsii*. In the *B. crocidurae* group, erythrocyte rosettes formed during spirochetemia blocked precapillary blood vessels and reduced the normal pattern of microcirculatory blood flow. After spirochetemia, erythrocyte rosettes disappeared and flow was normalized. Decreased blood flow and focal vascular damage with increased permeability and interstitial bleeding adjacent to the erythrocyte microemboli induced cell death in seminiferous tubules. Interestingly, we found that *B. crocidurae* could penetrate the tubules and remain in the testis long after the end of spirochetemia, suggesting that the testis can serve as a reservoir for this bacteria in subsequent relapses. The group infected with *B. hermsii* displayed normal testicular blood flow and vasomotion at all selected time points, and suffered no testicular damage. These results confirmed our hypothesis that the erythrocyte rosettes produce vascular obstruction and are the main cause of histopathology seen in model animal and human infections.

Key words: erythrocyte rosettes • laser Doppler flowmetry • testis • in vivo microscopy • hemorrhage

Introduction

Borrelia spirochetes, the causative agent of relapsing fever, are transmitted to mammalian hosts primarily by various species of soft-shelled ticks (*Argasidae*; references 1 and 2). After a bite from an infected tick, patients may experience one or more cycles of spirochetemia that induce the characteristic disease symptoms (3–5). This disease pattern is caused by the ability of relapsing fever *Borrelia* species to undergo antigenic variation. In particular, this pattern has been associated with the change of a surface lipoprotein called variable major protein (VMP) (6–8).

Borrelia crocidurae, the causative agent of African relapsing fever, uses an additional method to prolong its stay in the circulatory system of infected mammals. By inducing the formation of erythrocyte rosettes (erythrocyte aggregates), *B. crocidurae* escapes detection during immune surveillance (9). When mice were experimentally infected with *B. crocidurae*, microemboli formed by a combination of erythrocytes, spirochetes, and leukocytes were observed in several organs (10). Adjacent to these emboli, focal tissue damage with associated hemorrhage, cell death, and inflammation were also detected (10). These initial observations suggest to us that spirochete erythrocyte rosettes might be a significant factor in *B. crocidurae*–induced tissue damage. In addition, the endothelium is stimulated during *B. crocidurae* infection, leading to upregulation of adhesion molecules on the endothelium and promotion of transendothelial migration of neutrophils (11). This might be a key pathophysiologic mechanism in *B. crocidurae*–induced vascular damage.

In this paper, we investigate whether or not the erythrocyte spirochete rosettes, observed ex vivo in blood samples during spirochetemia, block the microcirculation in vivo, or are dissolved when passing the microvessels. Our approach compares in vivo testicular microcirculation be-

The online version of this article contains supplemental material.

A. Shamaei-Tousi's present address is Karolinska Institutet, Microbiology and Tumor Biology Center, S-171 77 Stockholm, Sweden.

Address correspondence to S. Bergström, Dept. of Microbiology, Umeå University, SE-901 87 Umeå, Sweden. Phone: 46-90-785-6726; Fax: 46-90-772-630; E-mail: sven.bergstrom@micro.umu.se

tween animals infected with *B. crocidurae* and *Borrelia hermsii*. We include *B. hermsii* in the study because this species does not form erythrocyte rosettes, and so serves as a useful control. We use the testis as the model organ, as it is easily accessible in the scrotum, and has a thin, transparent capsule, allowing direct studies of microcirculation in a nonmanipulated vascular bed with laser Doppler flowmetry (12–16) or with in vivo microscopy techniques after intravascular injection with fluorescent macromolecules (17). We develop a new animal model (rats) for studying this question that allows easy examination of organ microcirculation in vivo during the different phases of *B. crocidurae* infection. Rats infected with *B. crocidurae* display concomitant spirochetemia and symptoms resembling those of clinical infections (10, 18–22).

The functional consequences of disturbances in testicular microcirculation are well known (12), and immature germ cells are particularly susceptible to moderate reductions in blood flow (16). In the following experiment, we showed that the erythrocyte rosettes formed by *B. crocidurae* block pre- and postcapillary blood vessels, and that this blocking is likely to be of major biological relevance for the pathogenesis of organ damage during the infection. We also showed that *B. crocidurae* penetrate the seminiferous tubules and may remain there for prolonged periods, thus serving as a reservoir for systemic reinfection.

Materials and Methods

Animals and Bacterial Strains. The relapsing fever borreliae used in this study, *B. hermsii* HS1, serotype 7 (American Type Culture Collection no. 35209) and the initial isolate of *B. crocidurae*, were obtained from the strain collection of Alan G. Barbour (University of California Irvine College of Medicine, Irvine, CA).

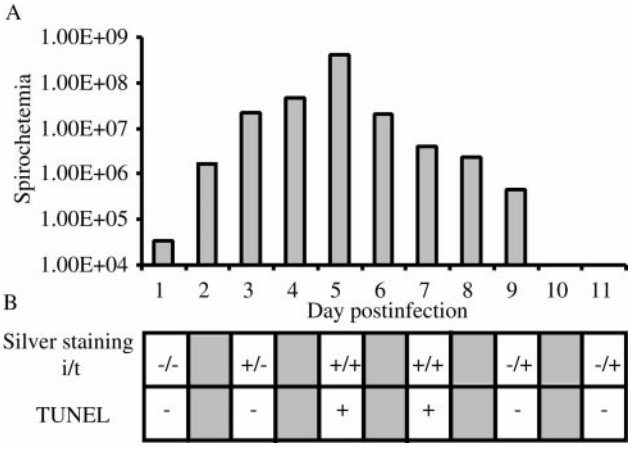

Figure 1. Summary of events during early *B. crocidurae* infection in rats. (A) Spirochetes in the blood were counted by light microscopy at ×400 magnification and displayed in logarithmic scale (error bars are omitted for clarity); (B) detection of borreliae by silver staining in the interstitial (i) and tubular (t) compartments of the testis are marked by (+) presence or (−) absence. TUNEL assay for detection of cell death of germ cells in tissue sections: (+) increased cell death; (−) no cell death. Five rats infected with *B. crocidurae* were examined at each time point.

Table I. *Total Body Weight of Rats Infected with B. crocidurae*

	Mean body weight	
	Not infected	Infected
	g	*g*
Day 0	374 ± 6.519	378 ± 5.701
Day 3	359 ± 7.416	359 ± 10.247
Day 5	355 ± 9.354	327 ± 11.511*
Day 11	363 ± 4.183	377 ± 10.368

Five rats were studied at each time point.
*$P \leq 0.0001$.

Adult male Sprague Dawley rats (300–350 g) were kept in a controlled laboratory environment, with food and water available ad libitum. All rats were anesthetized with pentobarbital (40 mg/kg) by a single intraperitoneal injection, and during each experiment kept supine on a heating pad.

Experimental Infections. Rats were inoculated with ~10^6 of *B. crocidurae* or *B. hermsii* suspensions into the peritoneal cavity. Development of spirochetemia was monitored by dark-field microscopy of a blood sample taken from the tail vein as described previously (10). In brief, whole blood samples from infected rats were diluted 1:10 with PBS and counted using a Petroff-Hausser chamber. Borreliae were cultured from testicular tissue at 34°C in BSKII medium (Sigma-Aldrich) complemented with 10% rabbit serum and 0.7% gelatin (23).

Testicular Microcirculation. At various time intervals after inoculation, rats were anesthetized and their testes exposed via a scrotal incision. Testicular microcirculation (flow level and pattern) was measured by laser Doppler technique as described previously (24, 25). In brief, the testis was immobilized in a plastic holder and embedded in 3% agar to prevent movement that would generate artifacts in the laser signal. A laser Doppler probe (PF 412; Perimed) was placed ~1 mm above the surface of the middle part of the testis not covered by agar, and testicular blood flow (in arbitrary perfusion units; PFUs)[1] was measured using a laser Doppler flowmeter (PF 4001; Perimed). The probe measures microvascular flow in a tissue volume of ~2–4 mm^3 below the laser probe. After observation of a stable blood flow, the signals were recorded for at least 10 min. The flow signals (mean flow in PFUs, vasomotion amplitude and frequency) were recorded and analyzed using the Perisoft v.5.10 software (Perimed).

In vivo microscopy of testicular microcirculation was performed as follows: in uninfected animals used as controls, and at 3 and 5 d after inoculation, rats were anesthetized and their testes exposed via a scrotal incision. The rats were placed on a microscope stage under an epifluorescence microscope objective. The tail artery was canulated and 150–200 μl of 5% macromolecular FITC-labeled dextran 150 (Sigma-Aldrich), suspended in PBS, was injected intraarterially (17). This high molecular weight FITC-labeled solution remained in the circulatory system after injection, causing circulating blood to fluoresce and allowing easy detection of blood vessels. The testicular microcirculation was then studied in vivo as described previously (17). In brief, the tes-

[1]*Abbreviations used in this paper:* IFV, interstitial fluid volume; PFU, arbitrary perfusion unit.

Table II. *Testes Weight of Rats Infected with B. crocidurae*

	Mean testes weight and interstitial fluid weight	
	Total weight of testes	Testicular intestinal fluid
	g	*g*
Day 0	1.926 ± 0.0357	0.12996 ± 0.00696
Day 3	1.862 ± 0.0428*	0.07204 ± 0.00657‡
Day 5	1.954 ± 0.0674	0.12456 ± 0.00995
Day 11	1.915 ± 0.0402	0.13096 ± 0.00749

Five rats were studied at each time point.
*$P \leq 0.001$.
‡$P \leq 0.01$.

ticular surface was overlayed with a cover glass and microcirculation was recorded by a video camera connected to a fluorescence microscope. This arrangement allowed both direct observation of testicular microcirculation on a monitor screen and subsequent analysis (17).

Testicular Interstitial Fluid Volume. At different time intervals after inoculation, rats were anesthetized for testes removal and testicular interstitial fluid volume (IFV) was measured as described (26). In brief, a small incision was made in the capsule, avoiding the underlying seminiferous tubules. Interstitial fluid was allowed to drip out of the testis for 16 h into a small vial and the weight of fluid was then recorded. Changes in the volume of testicular interstitial fluid directly reflect altered testicular blood flow and vascular permeability (12).

Testicular Histology. At different time intervals after inoculation, rats were killed and their testes removed. Each organ was weighed before fixation in 4% formaldehyde and embedding in paraffin. General testis morphology was examined using light microscopy of 5-μm thick sections stained with hematoxylin and eosin.

Terminal Transferase–mediated dUTP Nick End Labeling Assay. Cells with fragmented DNA were identified using a commercially available terminal transferase (TdT)-mediated dUTP nick end labeling (TUNEL) kit: the in situ Cell Death Detection kit (Boehringer [27]). In brief, 5-μm thick sections were cut after a 10-min treatment with proteinase K and incubated at 37°C with TdT for 60 min, as described previously (16). The slides were scored in a blinded fashion and the average number of TUNEL-positive cells per tubule cross section was counted in 100 randomly chosen tubules per testis.

Histological Detection of Borrelia in the Testis. Paraffin-embedded testis sections were stained with Dieterle silver to specifically detect spirochetes (10).

PCR Detection of Borrelia in the Testis. *Borrelia* DNA was extracted from different tissues as described previously (28), quantified, and then stored at −20°C. The *fla*B gene of *Borrelia* was used as the target for detecting *B. crocidurae* in tissues according to the method by Gebbia et. al. (29). Specific oligonucleotide primers used here were *fla*-1 5′-GCTCAAATTAGAGGATTATC-CCAAGC-3′ and *fla*-2 5′-GCATCTGAATATGTACCAT-TACCAG-3′. Each reaction contained 60 pmol of each primer, 2.5 U of *Taq* DNA polymerase (Amersham Pharmacia Biotech), 10 μl of 10× PCR buffer (100 mM Tris-HCl, pH 8.3, and 500 mM KCl), 20 μl of $MgCl_2$ (25 mM), 2.8 μl each of dATP and dTTP (10 mM), and 1.2 μl each of dCTP and dGTP (10 mM; all from Amersham Pharmacia Biotech). The cycling conditions were 15 s with initial denaturation at 94°C, followed by 45 cycles at 94°C (15 s), 67°C (30 s), and 72°C (15 s). At the end of 45 cycles, samples were held at 72°C for 7 min and stored at 4°C. Samples were concentrated in a Speed Vac (Savant) before analysis by electrophoresis on a 1% agarose gel. Negative controls included in this assay contained either no template DNA or template DNA prepared from uninfected mouse tissues.

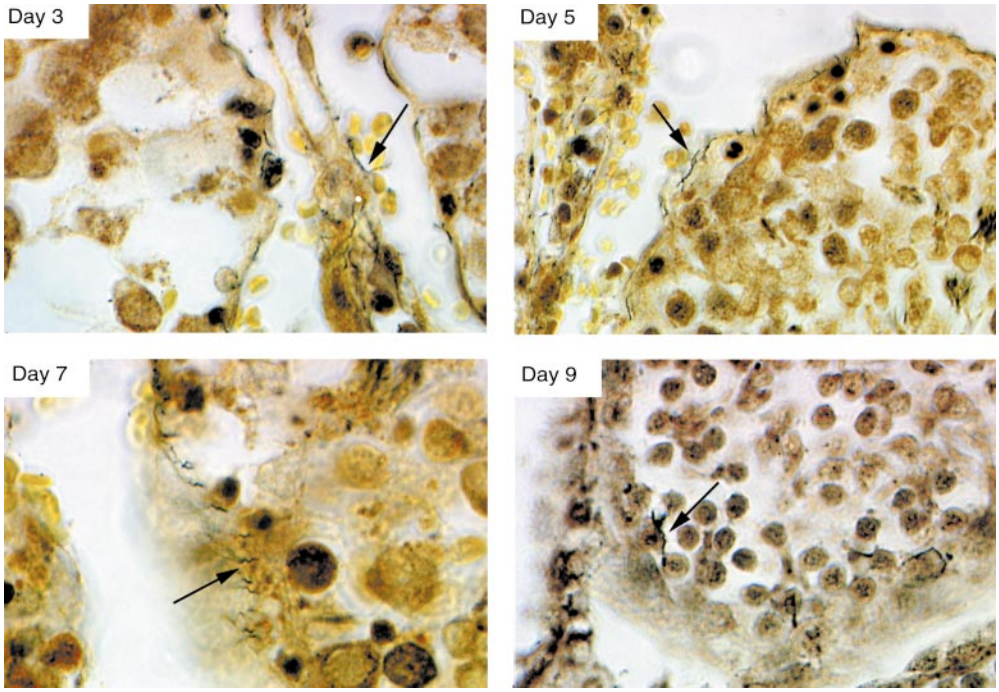

Figure 2. Testicular sections stained with a silver staining assay to detect spirochetes. 3 d after inoculation, *B. crocidurae* (arrows) were observed in the interstitium. 5 d after inoculation, attachment of the spirochetes to tubule walls was observed visually. 7 to 9 d after inoculation, migration of spirochetes to the inside of tubuli was observed and occasionally spirochetes were detected deep inside the tubules. Original magnification: ×1,000.

Statistics. Regression analysis, *t* test, and Mann-Whitney were used to show the statistical significance in the animal total weights and testes weights experiments.

Online Supplemental Material. The supplemental data is comprised of two video sequences from representative experiments depicted in Figs. 8 and 10. These experiments correspond directly to those used to prepare the still photos in Figs. 8 and 10 (see also the legends to Figs. 8 and 10). The videos are available at http://www.jem.org/cgi/content/full/193/9/995/F8/DC1 and http://www.jem.org/cgi/content/full/193/9/995/F10/DC1.

Results

Inoculation of Rats with the Relapsing Fever Agent B. crocidurae Led to Systemic Infection. Although various species of wild rodents in West Africa have been found infected with *B. crocidurae*, and this bacterium is a major cause of morbidity there (30), this study is, to our knowledge, the first to use a rat model to study *B. crocidurae* infection. Therefore, we began our work by first investigating the susceptibility of Sprague Dawley rats to this infection. Rats inoculated with *B. crocidurae* developed spirochetemia with one or two relapses (data not shown). During the primary spirochetemic phase (3–9 d after inoculation), at least 10^8 spirochetes per ml of blood were found, and rosette formation of erythrocytes by *B. crocidurae* was evident ex vivo. Collectively, these observations were similar to *B. crocidurae* infection in numerous murine models of infection (9, 10). 3 d after inoculation, the rats become spirochetemic with a peak 5 d after inoculation (Fig. 1 A). During the spirochetemic phase, rats displayed symptoms of ruffled fur, reluctance to move, head tilt, and a tendency to spin when lifted by the tail (data not shown). These characteristics were observed previously in a murine model of this infection (10). The body weight decreased 5 d after inoculation, but returned to baseline 2 d later (Table I). In this study using a rat model, testicular weight decreased 3 d after inoculation but later normalized (Table II). As shown previously by Bergh et al., the testicular volume is directly correlated to altered blood flow and vascular permeability (12). Testicular IFV per gram of testis decreased 3 d after inoculation, but was normal at the other time points studied (Table II). The decrease in IFV 3 d after inoculation was probably responsible for the decrease in total testis weight observed at the same

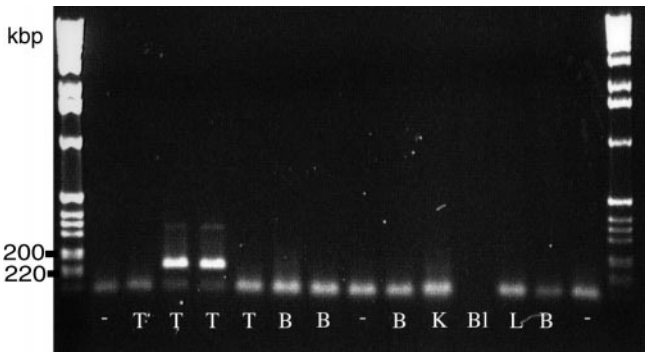

Figure 3. *B. crocidurae* DNA detection in testes. Testes (T), brain (B), kidney (K), blood (Bl), and lung (L) taken from rats 50 d after inoculation with *B. crocidurae* were dissected and probed for *Borrelia* DNA using PCR. The *fla*B gene was used as the target for detecting *B. crocidurae* in tissues. *B. crocidurae* DNA was found exclusively in the testis. The size, in kb, of the amplified fragments are given on the left. The figure is showing the testes and brain samples from four infected rats, together with a representative sample from other tissues from a sample rat. Each tissue was analyzed at least three times and similar results were obtained. DNA from uninfected tissue, marked as "−", served as control.

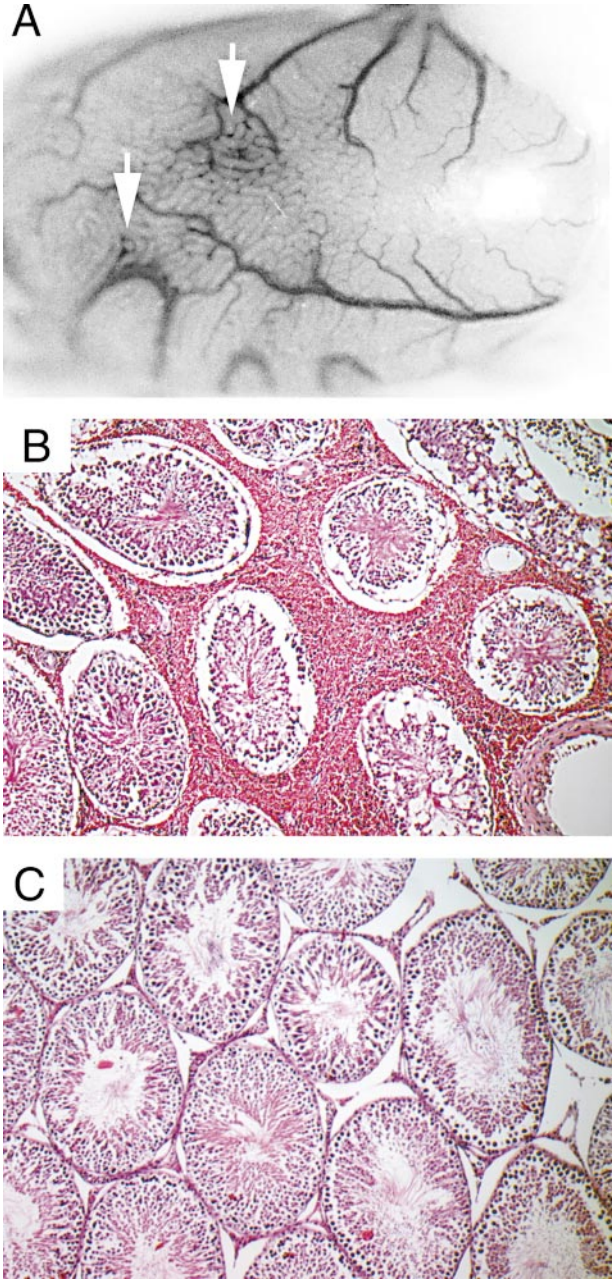

Figure 4. Histopathological changes in the testis during *B. crocidurae* infection. Interstitial bleeding (arrows) observed in the testes of *B. crocidurae*–infected animals at macroscopic (A) as well as microscopic (B) levels. Testes from rats infected with *B. hermsii* (C) did not show these pathologic lesions. Original magnifications: (A) ×3; (B and C) ×10.

time point. Similar to the rats infected with *B. crocidurae*, rats infected with the etiologic agent of North American relapsing fever, *B. hermsii*, also reached a level of 10^8 spirochetes per ml of blood during the peak of spirochetemia, which lasted for 1 d. In contrast, rats infected with nonerythrocyte rosetting *B. hermsii* displayed normal testicular blood flow and morphology at all time points (data not shown).

B. crocidurae Spirochetes Entered the Seminiferous Tubules and May Have Crossed the Blood–Testes Barrier. 3 d after inoculation, several *B. crocidurae* were detected in the interstitial space using a modified silver staining assay (Fig. 1 B and Fig. 2). 5 d after inoculation, spirochetes were observed attached to the seminiferous tubule walls, and sometime between days 7 and 9 the spirochetes migrated to the inside of the tubules. Spirochetes were detected in the outer layer of the tubules, and in some cases in more central positions, suggesting that some spirochetes had penetrated the blood–testes barrier (Fig. 2). In rats infected with *B. hermsii,* some spirochetes were observed in the interstitial space 3 to 7 d after inoculation; however, they were never observed inside the tubules (data not shown).

PCR was used to detect *B. crocidurae* spirochetes in tissues and blood isolated from infected animals without spirochetemia. Testis, brain, kidney, lung, and blood from rats infected with *B. crocidurae* were dissected and *Borrelia* DNA extracted. Surprisingly, when tissues were sampled 50 d after inoculation, among all the sampled tissues, only rat testes (two of four rats) were positive (Fig. 3). This suggests that spirochetes remained in the tubules of the testis. To investigate this further, we microdissected the tubular compartments of the rat testes 30, 50, and 60 d after inoculation with *B. crocidurae*. Analysis by light microscopy identified *B. crocidurae* spirochetes in the tubules both at 30 and 50 d after inoculation (data not shown).

Infection with B. crocidurae Resulted in Microvascular Damage and Interstitial Bleeding in the Testis. Foci of macroscopical bleeding were routinely seen when the testes were removed from infected rats (Fig. 4 A). These foci were representative of interstitial bleeding that contained extravasated erythrocytes and polymorph nuclear leukocytes (Fig. 4 B). Such interstitial hemorrhaging was initially observed 3 d after inoculation, with a peak in the number of hemorrhagic foci occurring on days 5 and 7. Foci rapidly disappeared 9 d after inoculation. The interstitial bleeding sites were generally observed adjacent to blood vessels with intravascular aggregates composed of erythrocytes, spirochetes, and some polymorphonuclear leukocytes (Fig. 5). 3 d after inoculation, occasional microemboli were seen in both the precapillary and postcapillary parts of the rat testes (Fig. 5, A and B) whereas later in the infection when emboli were more common, the latter were observed in the venous parts (Fig. 5, C and D). These microemboli corresponded to blood cell rosettes that blocked individual microvessels in the in vivo microscopy study (see below).

The general morphology of the seminiferous tubules was unaffected at all time points examined. In the control group, rats infected with nonerythrocyte rosetting *B. hermsii* showed no sign of histopathology of the testes (Fig. 4 C).

B. crocidurae Infection Induced Cell Death Among Germ Cells in the Seminiferous Tubules. Using the TUNEL assay, we observed an increase in the number of labeled germ cells,

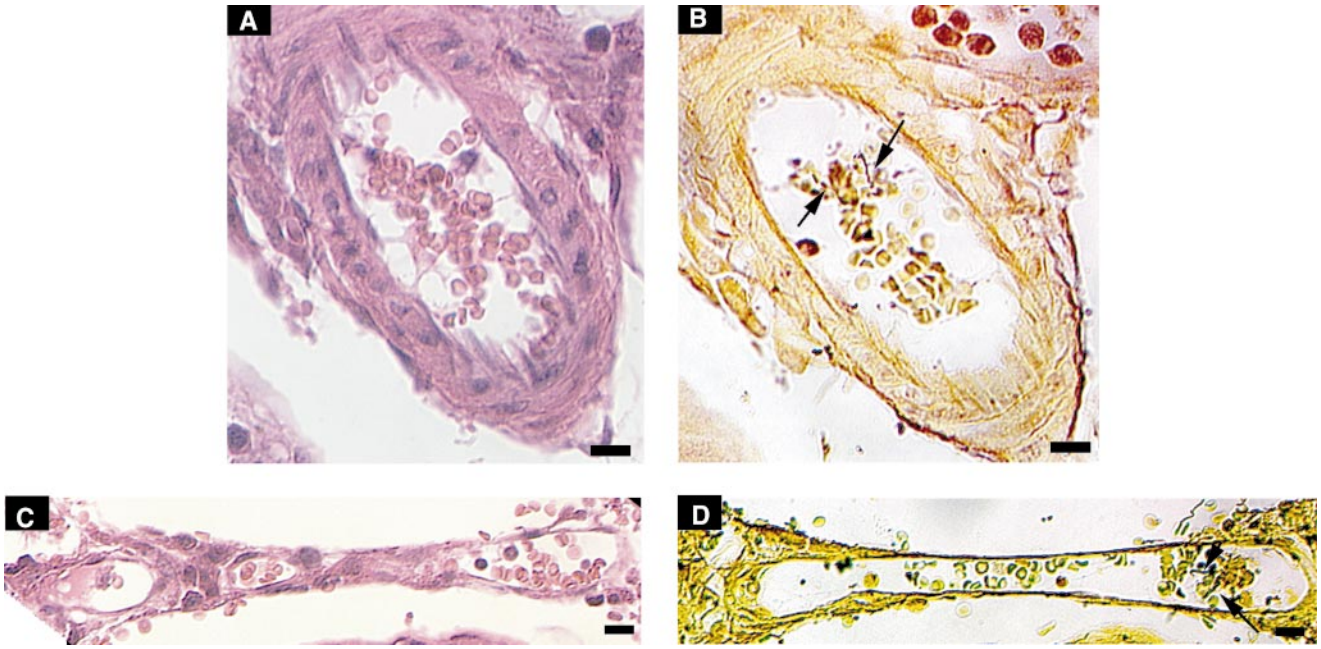

Figure 5. Localization of microemboli during *B. crocidurae* infection. Each row represents the same part of a section stained with eosin (A and C) or with modified silver staining (B and D). The top row is 3 d after inoculation, the bottom row 5 d after inoculation. In A and B, erythrocyte rosettes can be seen in a small artery, whereas in C and D erythrocyte rosettes can be seen in a postcapillary venule. Arrows point to spirochetes. Bars = 10 μm.

principally spermatogonia and spermatocytes, in the periphery of the seminiferous tubules 3 d after inoculation. However, a marked increase in cell death was detected 5 d after inoculation (Fig. 1 B and Fig. 6, A and C). Subsequently, the number of TUNEL-positive germ cells steadily declined at later time points until normality was reached 11 d after inoculation (Fig. 6 C). As a control, testes from rats infected with the nonerythrocyte rosetting *B. hermsii* displayed TUNEL-positive tubuli cells at the same frequency as uninfected control rats (Fig. 6 B).

B. crocidurae Infection Disturbed Testicular Microcirculation. In control rats, testicular microcirculation was characterized by regular high amplitude variations in blood flow known as vasomotion (Fig. 7 A), as described (12). However, 3 d after inoculation with *B. crocidurae,* total blood flow was slightly decreased and the vasomotion pattern irregular (Fig. 7 A). 5 to 7 d after inoculation, during the spirochetemic peak (Fig. 1), blood flow was reduced and vasomotion totally inhibited. However, 9 d after inoculation, irregular vasomotion had returned. Blood flow and vasomotion were fully normalized 11 d after inoculation (Fig. 7 A). Vasomotion and testicular blood flow were disturbed at time points corresponding to the presence of spirochete erythrocyte aggregates in the blood stream. This correlation supports a direct relationship between the effect on flow and the number of spirochetes present in the blood (Fig. 1). The maximal reduction in flow (40% of the normal value) was seen at the peak of spirochetemia, 5 d after inoculation (Fig. 7 B).

To further evaluate the effects of *B. crocidurae* infection, we studied testicular microcirculation in vivo 3 and 5 d after inoculation (Fig. 8, see also online supplemental video 1). Directly after intraarterial injection of FITC-labeled macromolecular dextran in control animals, the testicular microvessels were easily seen using fluorescence microscopy. The injected dextran remained in the circulatory system during the entire 30-min study period (data not shown). Rhythmical variations of flow in single microvessels were observed in single capillaries, and these were the basis for the oscillatory blood flow pattern (vasomotion) observed in normal testes with the laser Doppler (12). In contrast, the microcirculatory flow was generally slower in infected animals than in controls, and no rhythmical variations in flow were observed. In addition, distinct sites of leakage of fluorescent blood plasma were observed along the microvessels (Fig. 9). This leakage was evident principally in postcapillary vessels with a diameter of ~40–50 μm. Leakage of fluorescent dextran induced fluorescence of the whole interstitium after ~30 min, which prevented visual monitoring of the blood vessels. Circulating rosettes of erythrocytes were observed in the arteries, and trapped rosettes were occasionally seen in small precapillary vessels with a diameter size of 20–30 μm. Erythrocyte rosettes were also observed in postcapillary venules. Microvascular blood flow was abolished by such microemboli, as the vessel was nonfluorescent distally towards the block (Fig. 10, see also online supplemental video 2). Leakage sites and

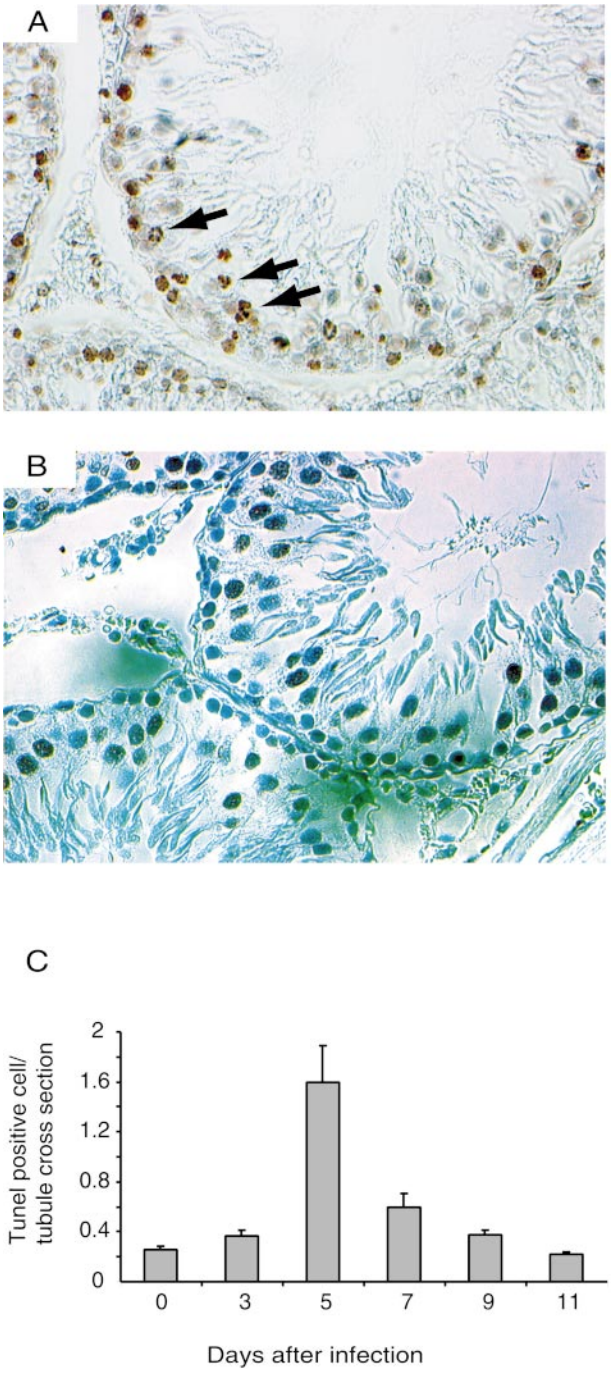

Figure 6. Induction of cell death among germ cells. Detection of cell death was performed using the TUNEL method. Tissue sections of tubules of testes of *B. crocidurae*–infected rats contained TUNEL-positive germ cells (arrows) between 3 and 9 d after inoculation (A and C). Quantification (number of TUNEL-positive cells per tubule cross-section) showed that the cell death peaked 5 d after inoculation (C). In testes from rats infected with the nonerythrocyte rosetting *B. hermsii*, no increase in TUNEL-positive germ cells was observed (B). Five rats were studied at each time points and bars show SDs. Original magnifications: (A and B) ×400.

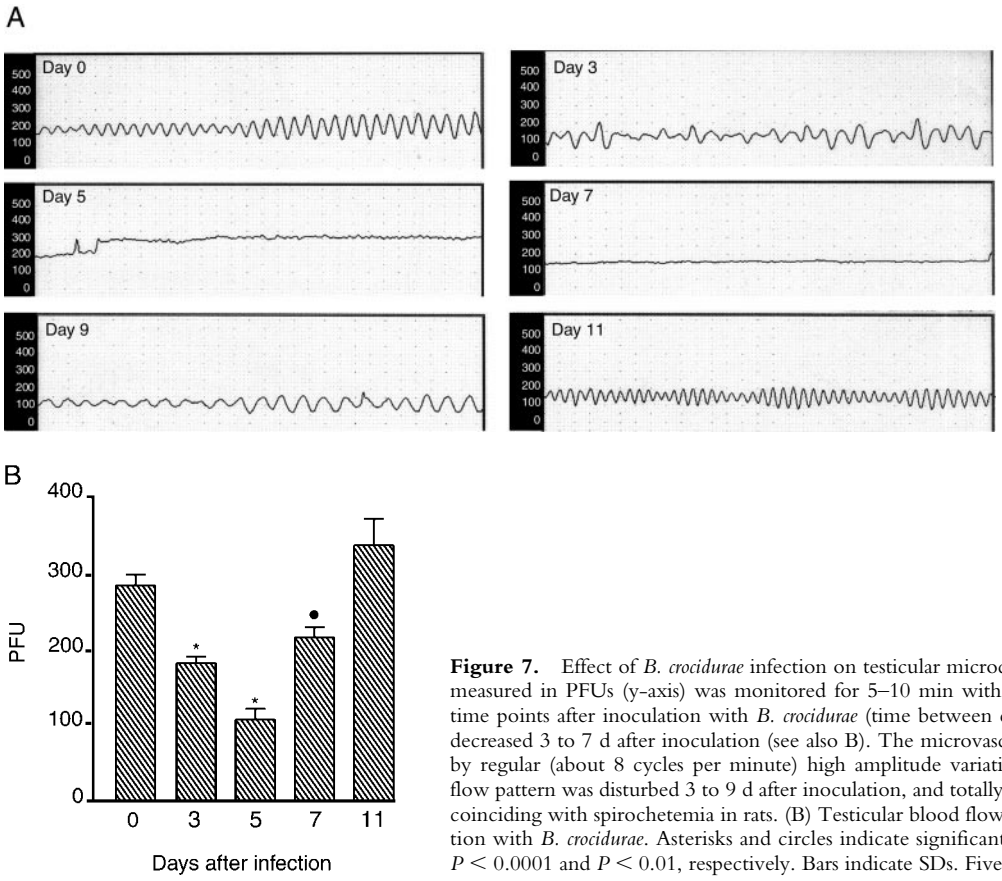

Figure 7. Effect of *B. crocidurae* infection on testicular microcirculation. (A) Testicular blood flow, measured in PFUs (y-axis) was monitored for 5–10 min with laser Doppler flowmetry at different time points after inoculation with *B. crocidurae* (time between dots along x-axis = 10 s). Total flow decreased 3 to 7 d after inoculation (see also B). The microvascular flow in the testis is characterized by regular (about 8 cycles per minute) high amplitude variations, termed vasomotion. This blood flow pattern was disturbed 3 to 9 d after inoculation, and totally abolished 5 and 7 d after inoculation, coinciding with spirochetemia in rats. (B) Testicular blood flow at different time points after inoculation with *B. crocidurae*. Asterisks and circles indicate significant differences from day 0 (control), by $P < 0.0001$ and $P < 0.01$, respectively. Bars indicate SDs. Five rats were studied at each time point.

vessels containing microemboli were significantly more predominant 5 d after inoculation compared with 3 d.

Discussion

An intriguing observation from this study is that *B. crocidurae* could penetrate the seminiferous tubules and remain there for extended periods, which may have contributed to tubule damage. However, because the peak in germ cell death was observed before the detection of spirochetes inside the tubules, it is likely that altered blood flow was a more important factor in germ cell death, as this feature paralleled the appearance of tubule damage. The testis is an immune-privileged site where immune reactions are continuously suppressed in order to avoid autoimmune reactions against germ cells that are potent antigens (31). Therefore, the seminiferous tubule is not an unlikely reservoir for *B. crocidurae* spirochetes. Thus, like the brain (10, 18, 19, 29), the testis may serve as a reservoir for *B. crocidurae*. Recently, it was also suggested that migratory restlessness in redwing thrushes might trigger new spirochetemia by releasing spirochetes from such reservoirs (32). It would

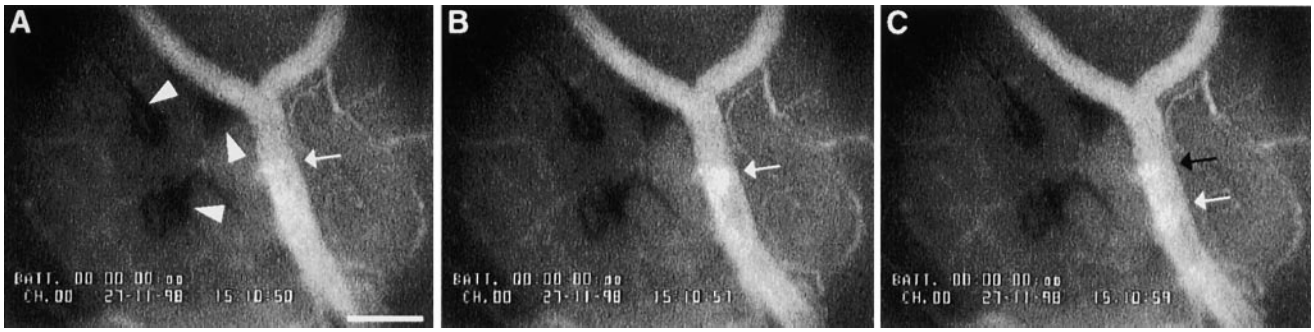

Figure 8. Identification of blood cells aggregates in microvessels of infected rats. A–C illustrate the same vascular field within the rat testes after 3 d of *B. crocidurae* infection, before injection of FITC-dextran. A slowly moving aggregate of blood cells is indicated by a white arrow. C depicts a new aggregate of blood cells (black arrow). A and B are separated by 7 s and B and C by 2 s. The panels also show interstitial bleeding (arrowheads) around blood vessels of testes. Video illustrating the figures is explained in the supplemental video 1; bar = 166 μm.

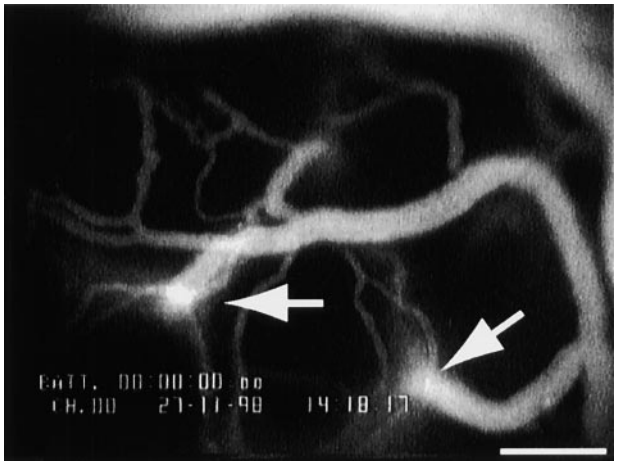

Figure 9. Fluorescence micrographs of testicular microcirculation in *B. crocidurae*–infected animals. After intraarterial injection of FITC-labeled dextran, the microvasculator of testes of *B. crocidurae*–infected rat were easily seen by fluorescence microscopy. Leakage of FITC-dextran (arrows) was observed as a consequence of distal microemboli formation in the vessel. The testes were photographed 15 min after injection of FITC-dextran; bar = 166 μm.

be of interest to test such a hypothesis by inducing stress (i.e., hormonal or physical) in rats that have been infected with *B. crocidurae* but are asymptomatic and thereby reactivating a latent *Borrelia* infection. Similarly to *B. crocidurae*, the syphilis spirochete, *Treponema pallidum*, also colonizes the testicular interstitium (33). In contrast to *T. pallidum*, *B. crocidurae* is also able to penetrate the seminiferous tubules. To our knowledge, this is the first report showing that a pathogenic bacterium could take advantage of the testes as a site for a possible systemic reinfection. Besides being an immune-privileged organ, the testicular milieu with its relatively low temperature could be attractive for borreliae species with their low optimal cultivation temperature.

In our experiment, erythrocyte rosettes blocked pre- and postcapillary blood vessels and completely stopped blood flow in the affected vessels. This result demonstrates that at least some of the rosettes observed in blood samples ex vivo have the physical properties in vivo to block microcirculatory blood flow. We also noted that dextran leaked from these vessels, demonstrating a major increase in vascular permeability that is probably caused by vascular damage. Analysis of infected tissue sections confirmed the presence of blood vessels with microemboli formed by a combination of erythrocytes, spirochetes, and leukocytes. Adjacent to these structures was concomitant interstitial hemorrhage. The number of vessels blocked by erythrocyte-rosettes was proportional to the number of spirochetes in the blood, the largest number of blocked vessels being seen 5 d after inoculation, the peak of the spirochetemia. Using laser Doppler flowmetry, we demonstrated that blockage of microvessels with microemboli was sufficient to reduce blood flow by 60% 5 d after inoculation. A decrease of this magnitude would clearly induce death among germ cells in the seminiferous tubules, as a 30% reduction of blood flow during a 5-h period, caused by a partial ligation of the testicular artery, induced focal apoptosis among the spermatogonia and spermatocytes, and a further decrease induced necrotic cell death in the seminiferous tubules in rats (16). Also in this study the increase in TUNEL-positive dying germ cells was proportional to disruption of testicular blood flow. Therefore, we conclude that the erythrocyte spirochete rosettes, formed in the blood during spirochetemia in animals infected with *B. crocidurae*, cause tissue damage by forming emboli in microvessels. In contrast, there was an absence of microcirculatory disturbances or testis damage in rats infected with the nonerythrocyte rosetting *B. hermsii*.

In a previous study, SCID mice infected with *Borrellia turicatae*, a causative agent of North American relapsing fever, had numerous spirochetes in their testicular fluid but no inflammation of their testes (18). This correlates with our finding that *B. hermsii*–infected rats are not likely to induce pathological changes in the testes. Thus, erythrocyte rosetting induced by *B. crocidurae* was the main reason for altered blood flow and testicular damage in infected rats.

The testicular microcirculatory system in rats is characterized by regular, high amplitude vasomotion (12). Rhythmical variations in microvascular flow are caused by

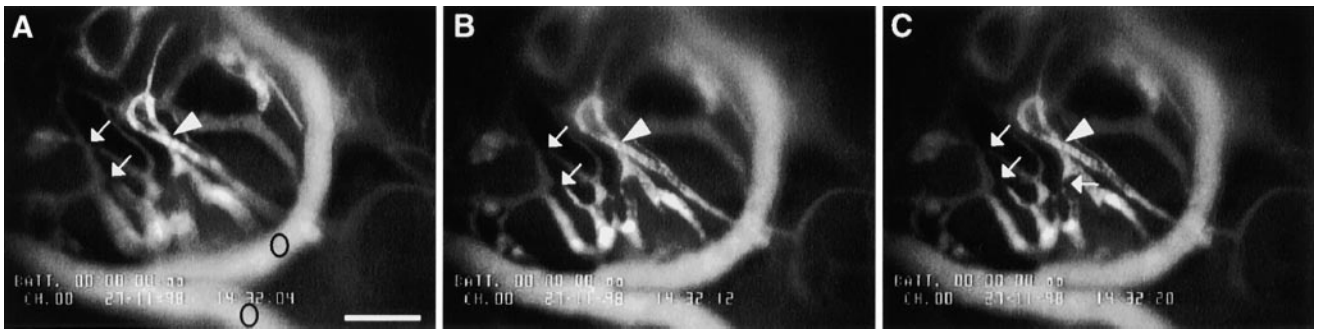

Figure 10. Identification of microvasculatory plugs in testes of infected rats by fluorescence-labeled dextran. A–C illustrate the same vascular field within the rat testes after 5 d of *B. crocidurae* infection, after injection of FITC-dextran. The nonfluorescent area of the microvessels indicates a blockage of the vessels as a result of microemboli formation (arrows). The arrowheads point at the areas of no blood flow, because the blood vessels were nonfluorescent distally towards the blockage. Circles in panel A indicate two vessels with normal flow. A and B are separated by 8 s and B and C by 8 s. Video illustrating the figures is explained in the online supplemental video 2. The testes were photographed 15 min after injection of FITC-dextran; bar = 166 μm.

spontaneous myogenic activity in precapillary blood vessels (34), and are necessary to promote movement of plasma from the interstitial space back into postcapillary venules during phases with slow flow (12). We demonstrated previously that physiological factors (i.e., hormones) as well as pathological factors (i.e., cigarette smoking) disturb this aspect of testicular microcirculation (12, 35). We now extend these findings to include the presence of microemboli in small arteries, occurring in early stages of spirochetemia, as a factor for impaired testicular vasomotion.

During the experiment, we also observed differences in the frequency of erythrocyte rosetting at various sites. The majority of rosettes were observed in the postcapillaries and venules, whereas relatively few were seen in the arterioles. It is known that the highest erythrocyte velocities and wall shear rates are in the arterioles. These rates drop significantly when the erythrocytes migrate from the capillaries to the immediate postcapillary venules, before rising again in the larger venules (36). Consequently, although high flow rates in the arterioles make it difficult for rosette formation, slower flow rates in the immediate postcapillary venules provide ample opportunities for rosette formation. This suggests that most of erythrocyte rosettes were disrupted when migrating through the capillary part of the blood system, as erythrocytes can pass through the capillaries only as single cells. Therefore, we conclude that the erythrocyte rosettes must have been reestablished in the postcapillary part of the blood system.

The preferred sites of erythrocyte rosettes caused by *B. crocidurae* infection are thus similar to those caused by *Plasmodium falciparum*, the agent of cerebral malaria (37, 38). Using artificially perfused rat mesocecum vasculature, it was demonstrated that these rosettes too are restricted to venules, especially in areas of slow blood flow.

Testicular weight was lowered 3 d after inoculation but unaffected at all other time points. Presumably, this reduction was caused by a transient decrease in testicular IFV at that time point. The interstitial tissues of rat testes contain large fluid-filled lymphatic sinusoids. Significant changes in fluid volume in these regions are caused by changes in flow and vascular permeability (12). Thus, the drop in IFV 3 d after inoculation was probably caused by the combination of decreased flow and filtration due to microembolization. Moreover, testis weight and IFV were not reduced at the later time points probably because the effect of decreased flow was counteracted by increased permeability and incidence of focal interstitial hemorrhages.

Studying microcirculatory flow with a combination of laser Doppler and in vivo microscopy is a sensitive method to monitor changes in microcirculation and its relationship to tissue damage induced by conditions of blood-borne infections or other factors leading to the formation of erythrocyte "plugs". An especially promising application of this method might be the study of *Plasmodium* species, the causative agent of malaria in the vascular system. Malaria-infected erythrocytes display features similar to those induced by the presence of *B. crocidruae* in blood systems, although the rosetting properties are presented on the surface of infected erythrocytes instead of the parasite itself (39–42). Thus, using in vivo microscopy and laser Doppler flowmetry might facilitate investigation of efficient antirosetting therapies.

We thank Paul Haemig and Matthew Francis for critically reading the manuscript, Per Arnqvist for statistical consultation, and Ingela Nilsson, Sigrid Kilter, Elisabeth Dahlberg, and Birgitta Ekblom for their skillful technical assistance.

This study was supported by the Swedish Medical Research Council (projects 07922 and 05935), the J. C. Kempes Foundation (grant to A. Shamaei-Tousi), and the Maud and Birger Gustavsson Foundation.

Submitted: 28 November 2000
Revised: 5 March 2001
Accepted: 21 March 2001

References

1. Burgdorfer, W. 1976. The epidemiology of the relapsing fevers. *In* The Biology of Parasitic Spirochetes. R.C. Johnson, editor. Academic Press, New York. 191–200.
2. Felsenfeld, O. 1968. *Borrelia*: Strains, Vectors, Human and Animal Borreliosis. Warren H. Green, St. Louis, MO. 180 pp.
3. Barbour, A.G. 1990. Antigenic variation of a relapsing fever *Borrelia* species. *Annu. Rev. Microbiol.* 44:155–171.
4. Barbour, A.G. 1993. Linear DNA of *Borrelia* species and antigenic variation. *Trends Microbiol.* 1:236–239.
5. Wilske, B., A.G. Barbour, S. Bergström, N. Burman, B.I. Restrepo, P.A. Rosa, T. Schwan, E. Soutschek, and R. Wallich. 1992. Antigenic variation and strain heterogeneity in Borrelia spp. *Res. Microbiol.* 143:583–596.
6. Stoenner, H.G., T. Dodd, and C. Larsen. 1982. Antigenic variation of *Borrelia hermsii*. *J. Exp. Med.* 156:1297–1311.
7. Barstad, P.A., J.E. Coligan, M.G. Raum, and A.G. Barbour. 1985. Variable major proteins of *Borrelia hermsii*. Epitope mapping and partial sequence analysis of CNBr peptides. *J. Exp. Med.* 161:1302–1314.
8. Burman, N., S. Bergström, B.I. Restrepo, and A.G. Barbour. 1990. The variable antigens Vmp7 and Vmp21 of the relapsing fever bacterium *Borrelia hermsii* are structurally analogous to the VSG proteins of the African trypanosome. *Mol. Microbiol.* 4:1715–1726.
9. Burman, N., A. Shamaei-Tousi, and S. Bergström. 1998. The spirochete *Borrelia crocidurae* causes erythrocyte rosetting during relapsing fever. *Infect. Immun.* 66:815–819.
10. Shamaei-Tousi, A., P. Martin, A. Bergh, N. Burman, T. Brännström, and S. Bergström. 1999. Erythrocyte-aggregating relapsing fever spirochete *Borrelia crocidurae* induces formation of microemboli. *J. Infect. Dis.* 180:1929–1938.
11. Shamaei-Tousi, A., M.J. Burns, J.L. Benach, M.B. Furie, E.I. Gergel, and S. Bergström. 2000. The relapsing fever spirochaete, *Borrelia crocidruae* activates human endothelial cells and promotes the transendothelial migration of neutrophils. *Cell. Microbiol.* 2:591–599.
12. Bergh, A., and J.E. Damber. 1993. Vascular controls in testicular physiology. *In* Molecular Biology of the Male Reproductive System. D. De Kretser, editor. Academic Press Inc., Orlando, FL. 439–468.
13. Bolognese, P., J.I. Miller, I.M. Heger, and T.H. Milhorat. 1993. Laser-Doppler flowmetry in neurosurgery. *J. Neuro-*

surg. Anesthesiol. 5:151–158.
14. Braverman, I.M. 1997. The cutaneous microcirculation: ultrastructure and microanatomical organization. *Microcirculation*. 4:329–340.
15. Oberg, P.A. 1990. Laser-Doppler flowmetry. *Crit. Rev. Biomed. Eng.* 18:125–163.
16. Bergh, A., O. Collin, and E. Lissbrant. 2001. Effects of acute graded reductions in testicular blood flow on testicular morphology in the adult rat. *Biol. Reprod.* 64:13–20.
17. Bergh, A., P. Rooth, A. Widmark, and J.E. Damber. 1987. Treatment of rats with hCG induces inflammation-like changes in the testicular microcirculation. *J. Reprod. Fertil.* 79: 135–143.
18. Cadavid, D., D.D. Thomas, R. Crawley, and A.G. Barbour. 1994. Variability of a bacterial surface protein and disease expression in a possible mouse model of systemic Lyme borreliosis. *J. Exp. Med.* 179:631–642.
19. Cadavid, D., and A.G. Barbour. 1998. Neuroborreliosis during relapsing fever: review of the clinical manifestations, pathology, and treatment of infections in humans and experimental animals. *Clin. Infect. Dis.* 26:151–164.
20. Aubry, P., J. Renambot, J. Teyssier, Y. Buisson, G. Granic, G. Brunetti, P. Dano, and P. Bauer. 1983. Borreliosis caused by ticks in Senegal; apropos of 23 cases. *Dakar Med.* 28:413–420.
21. Goubau, P.F. 1984. Relapsing fevers. A review. *Ann. Soc. Belg. Med. Trop.* 64:335–364.
22. Southern, P., and J. Sanford. 1969. Relapsing fever: a clinical and microbiological review. *Medicine*. 48:129–149.
23. Barbour, A.G. 1984. Isolation and cultivation of Lyme disease spirochetes. *Yale J. Biol. Med.* 57:521–525.
24. Collin, O., J.E. Damber, and A. Bergh. 1996. 5-Hydroxytryptamine--a local regulator of testicular blood flow and vasomotion in rats. *J. Reprod. Fertil.* 106:17–22.
25. Lissbrant, E., and A. Bergh. 1997. Effects of vasoactive intestinal peptide (VIP) on the testicular vasculature of the rat. *Int. J. Androl.* 20:356–360.
26. Widmark, A., J.E. Damber, and A. Bergh. 1986. Relationship between human chorionic gonadotrophin-induced changes in testicular microcirculation and the formation of testicular interstitial fluid. *J. Endocrinol.* 109:419–425.
27. Gavrieli, Y., Y. Sherman, and S.A. Ben-Sasson. 1992. Identification of programmed cell death in situ via specific labeling of nuclear DNA fragmentation. *J. Cell Biol.* 119:493–501.
28. Yang, L., J.H. Weis, E. Eichwald, C.P. Kolbert, D.H. Persing, and J.J. Weis. 1994. Heritable susceptibility to severe *Borrelia burgdorferi*-induced arthritis is dominant and is associated with persistence of large numbers of spirochetes in tissues. *Infect. Immun.* 62:492–500.
29. Gebbia, J.A., J.C. Monco, J.L. Degen, T.H. Bugge, and J.L. Benach. 1999. The plasminogen activation system enhances brain and heart invasion in murine relapsing fever borreliosis. *J. Clin. Invest.* 103:81–87.
30. Trape, J.F., J.M. Duplantier, H. Bouganali, B. Godeluck, F. Legros, J.P. Cornet, and J.L. Camicas. 1991. Tick-borne borreliosis in west Africa. *Lancet.* 337:473–475.
31. Hedger, M.P., J.X. Qin, D.M. Robertson, and D.M. de Kretser. 1990. Intragonadal regulation of immune system functions. *Reprod. Fertil. Dev.* 2:263–280.
32. Gylfe, Å., S. Bergström, J. Lundström, and B. Olsén. 2000. Reactivation of Borrelia infection in birds. *Nature.* 403:724–725.
33. Lukehart, S.A., S.A. Baker-Zander, and S. Sell. 1980. Characterization of lymphocyte responsiveness in early experimental syphilis. I. In vitro response to mitogens and Treponema pallidum antigens. *J. Immunol.* 124:454–460.
34. Damber, J.E., A. Bergh, B. Fagrell, O. Lindahl, and P. Rooth. 1986. Testicular microcirculation in the rat studied by videophotometric capillaroscopy, fluorescence microscopy and laser Doppler flowmetry. *Acta Physiol. Scand.* 126:371–376.
35. Collin, O., S. Kilter, and A. Bergh. 1995. Tobacco smoke disrupts testicular microcirculation in the rat. *Int. J. Androl.* 18:141–145.
36. Kaul, D.K., M.E. Fabry, and R.L. Nagel. 1989. Microvascular sites and characteristics of sickle cell adhesion to vascular endothelium in shear flow conditions: pathophysiological implications. *Proc. Natl. Acad. Sci. USA.* 86:3356–3360.
37. Raventos-Suarez, C., D.K. Kaul, F. Macaluso, and R.L. Nagel. 1985. Membrane knobs are required for the microcirculatory obstruction induced by *Plasmodium falciparum*-infected erythrocytes. *Proc. Natl. Acad. Sci. USA.* 82:3829–3833.
38. Kaul, D.K., E.F. Roth, Jr., R.L. Nagel, R.J. Howard, and S.M. Handunnetti. 1991. Rosetting of *Plasmodium falciparum*-infected red blood cells with uninfected red blood cells enhances microvascular obstruction under flow conditions. *Blood.* 78:812–819.
39. Udomsangpetch, R., B. Wahlin, J. Carlson, K. Berzins, M. Torii, M. Aikawa, P. Perlmann, and M. Wahlgren. 1989. *Plasmodium falciparum*–infected erythrocytes form spontaneous erythrocyte rosettes. *J. Exp. Med.* 169:1835–1840.
40. Carlson, J., and M. Wahlgren. 1992. *Plasmodium falciparum* erythrocyte rosetting is mediated by promiscuous lectin-like interactions. *J. Exp. Med.* 176:1311–1317.
41. David, P.H., S.M. Handunnetti, J.H. Leech, P. Gamage, and K.N. Mendis. 1988. Rosetting: a new cytoadherence property of malaria-infected erythrocytes. *Am. J. Trop. Med. Hyg.* 38:289–297.
42. Aikawa, M., M. Iseki, J.W. Barnwell, D. Taylor, M.M. Oo, and R.J. Howard. 1990. The pathology of human cerebral malaria. *Am. J. Trop. Med. Hyg.* 43:30–37.